Visual Neuroscience (2014), **31**, 177–187.
Copyright © Cambridge University Press, 2014 0952-5238/14 $25.00
doi:10.1017/S0952523813000631

SPECIAL ISSUE

Short Wavelength-Sensitive Cones and the Processing of Their Signals

REVIEW ARTICLE

Distribution and specificity of S-cone ("blue cone") signals in subcortical visual pathways

PAUL R. MARTIN[1,2] AND BARRY B. LEE[3,4]

[1]Department of Ophthalmology and Save Sight Institute, The University of Sydney, Sydney, New South Wales, Australia
[2]Australian Research Council Centre of Excellence in Vision Science, The University of Sydney, Sydney, New South Wales, Australia
[3]SUNY College of Optometry, New York, New York
[4]Max Planck Institute for Biophysical Chemistry, Göttingen, Germany

(Received August 30, 2013; Accepted December 12, 2013; First Published Online February 20, 2014)

Abstract

We review here the distribution of S-cone signals and properties of S-cone recipient receptive fields in subcortical pathways. Nearly everything we know about S-cone signals in the subcortical visual system comes from the study of visual systems in cats and primates (monkeys); in this review, we concentrate on results from macaque and marmoset monkeys. We discuss segregation of S-cone recipient (blue-on and blue-off) receptive fields in the dorsal lateral geniculate nucleus and describe their receptive field properties. We treat in some detail the question of detecting weak S-cone signals as an introduction for newcomers to the field. Finally, we briefly consider the question on how S-cone signals are distributed among nongeniculate targets.

Introduction and history

Among mammals, simian primates have the best-developed color vision. Humans, apes, and Old World monkeys show routine trichromatic color vision based on receptors sensitive to short, medium, and long wavelengths of light. We know from molecular biology that the short-wave sensitive (S) cones diverged from other cone types relatively early in the mammalian evolutionary history, whereas distinct long-wave (L) and medium-wave (M) pigments under the genetic control of X-chromosomes diverged in different primate species, at different times, during the course of evolution (Shyue et al., 1995; Nathans, 1999). The bases of these discoveries are reviewed elsewhere in this volume (Hunt & Peichl, 2013). As we note above (see Abstract section) and below, nearly everything we know about S-cone signals in the subcortical visual system comes from the study of visual systems in cats and primates (monkeys), and in this review, we concentrate on the results from macaque and marmoset monkeys, which are the species where most is known.

Early electrophysiological studies of color vision in central pathways began before or concurrent with significant discoveries on color vision evolution and genetics. The earliest experiments demonstrated color opponent properties in single cells but did not identify cone inputs or characterize spatial properties (DeValois, 1960; Hubel & Wiesel, 1960). Early recorders of single unit activity in monkey (usually macaque) retina and lateral geniculate nucleus (LGN)–treated S, M, and L cone inputs to receptive fields as potential inputs to a multidimensional system, where opponent inputs in different combinations (e.g., +S/−M; −S/+L; +M/−L) were equally likely (DeValois et al., 1966; Wiesel & Hubel, 1966; Gouras, 1968; DeMonasterio et al., 1975; Gielen et al., 1982; Creutzfeldt et al., 1986; Crook et al., 1987). It soon became apparent that among spectrally opponent cells, a class called "blue-on/yellow-off" (hereinafter referred to as blue-on) was more commonly encountered than its symmetric counterpart "yellow-on/blue-off" (hereinafter referred to as blue-off); this was especially true in the retina (Malpeli & Schiller, 1978; DeMonasterio, 1979; Valberg et al., 1986). A second concept derived from early work was that specific color-coding receptive fields exist that show spatially overlapping spectrally opponent "Type II" organization (Wiesel & Hubel, 1966; DeMonasterio & Gouras, 1975; Dreher et al., 1976). This assumption turns out to be reasonable in the case of blue-on cells (Tailby et al., 2008*a*,*b*; Crook et al., 2009), but the spatial and chromatic organization of red–green opponent cells turned out to be more variable and complex than expected (Lee et al., 1983, 2012; Derrington et al., 1984; Rodieck, 1991; Reid & Shapley, 2002; Diller et al., 2004; Martin et al., 2011). A final assumption of early work was that all color signals pass through the dorsal parvocellular layers of the LGN en route to the granular layers of primary visual cortex. This assumption is likely to be correct in the case of red–green opponent cells but as shown below is unlikely to be correct in the case of blue-on and blue-off cells.

Address correspondence to: Paul Martin, Save Sight Institute, Sydney Eye Hospital Campus, 8 Macquarie St, Sydney, New South Wales 2001, Australia. E-mail: prmartin@sydney.edu.au

https://doi.org/10.1017/S0952523813000631 Published online by Cambridge University Press

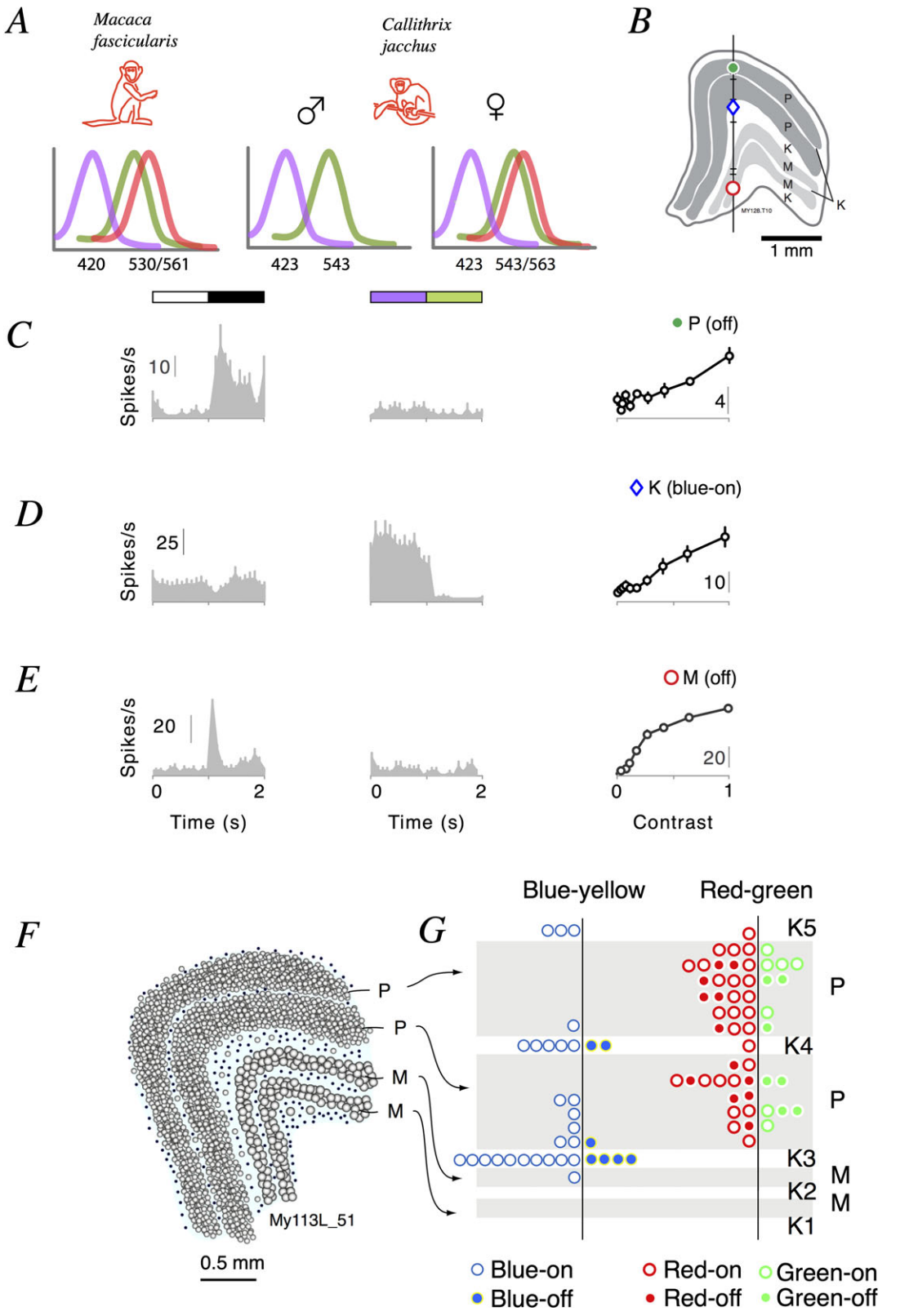


Fig. 1. Identification and distribution of short-wave sensitive (S) cone signals in the LGN. (**A**) Sketches of spectral sensitivity of cone photoreceptors in macaque monkey (left panel) and two color vision phenotypes of marmoset monkey (center and right panels). Numbers on wavelength axes show peak spectral sensitivities (nm). All monkeys express S-cones with peak sensitivity near 420 nm. Macaque monkeys show routine trichromatic color vision, expressing ML sensitive pigment with maxima near 530 nm (medium) and 561 nm (long). Marmoset monkeys show polymorphic color vision with three allelic variants of ML pigments with peak sensitivity near 543, 556 (not shown), and 563 nm. All males and females homozygous for the opsin alleles are dichromats (center panel), whereas heterozygous females express two ML pigments (right panel). (**B**) Drawing of a coronal section through marmoset LGN showing parvocellular (P, light

https://doi.org/10.1017/S0952523813000631 Published online by Cambridge University Press

Distribution of cone-opponent signals in LGN

Retrograde labeling studies in macaque and marmoset monkeys showed that the small bistratified (blue-on) cells project to the LGN (Rodieck & Watanabe, 1993; Dacey et al., 2003; Szmajda et al., 2008), and one prescient single-cell study in macaque LGN indicated blue-on cells were more commonly encountered in the deeper P layers than in the superficial P layers (Schiller & Malpeli, 1978). Here, we focus first on results from recordings in marmoset monkeys, since the koniocellular layers (where, it turns out, many blue-on receptive fields are found; see below) are relatively broad (Walls, 1953; Kaas et al., 1978) and targetable with an electrode (Martin et al., 1997). Fig. 1A compares the cone sensitivity in macaque monkey with examples of a male and female marmoset (*Callithrix jacchus*). Marmosets in common with most other New World monkeys show sex-linked polymorphism of color vision, whereby genes coding medium- and long-wavelength-sensitive pigments are present as allelic variants at a single locus on the X chromosome (reviewed by Mollon, 1989; Jacobs, 2008). Males are thus obligate dichromats, whereas females expressing different alleles on each X chromosome show red–green cone opponent receptive fields (Yeh et al., 1995*b*) and can make trichromatic color discriminations (Tovée et al., 1992). The differences between LGN responses in dichromatic and trichromatic marmosets are detailed elsewhere (Yeh et al., 1995*b*; Kilavik et al., 2003; Martin et al., 2011). Fig. 1B shows a drawing from a coronal section through marmoset LGN. The vertical line shows the path of an extracellular recording electrode, which passed through the parvocellular (P), koniocellular (K), and magnocellular (M) layers. Colored symbols mark the positions of three example receptive fields recorded on this path, short horizontal lines mark the positions of other recorded receptive fields. Peristimulus time histograms (PSTHs) and contrast-response functions of the three example cells are shown in Fig. 1C–1E. The P off-centre cell (Fig. 1C) shows a vigorous response to achromatic contrast decrement (left PSTH) but no response to S-cone contrast increments (center PSTH), indicating no functional input from S-cones to this receptive field. Responses to drifting (5 Hz) low spatial frequency achromatic grating presented at different contrasts were subjected to Fourier analysis, the resulting amplitude component at stimulus frequency (right column) shows the expected low gain and linear contrast-response function (Derrington & Lennie, 1984; Kaplan & Shapley, 1986; Crook et al., 1987; Croner & Kaplan, 1995; Kremers et al., 2004).

Responses of a blue-on cell recorded in koniocellular layer K3 (between the P and M layers) are shown in Fig. 1C. This cell shows negligible response to achromatic contrast but is strongly excited by S-cone contrast increments, indicating on-type excitation from S-cones to the receptive field (Derrington et al., 1984; Lee et al., 1987; Yeh et al., 1995*b*). Consistently, the contrast-response function for drifting S-cone isolating gratings shows linear dependence of response on S-cone contrast (Fig. 1C, right column). In addition to blue-on cells such as the one exemplified here, other receptive fields encountered in marmoset K layers included blue-off cells (Szmajda et al., 2006), "suppressed by contrast" cells (Solomon et al., 2010), orientation-tuned cells (Cheong et al., 2013), cells that otherwise resembled P cells in functional properties (likely displaced constituents of the P pathway), and cells with poor responsivity to any visual stimulus presented (White et al., 2001).

On passing from K layers to the M layers (Fig. 1D), the most commonly encountered receptive fields showed the expected transient responses to achromatic contrast (left PSTH), little or no functional input from S-cones (center PSTH), high achromatic contrast gain and saturating responses to high contrast levels (right column) (Derrington & Lennie, 1984; Kaplan & Shapley, 1986; Crook et al., 1987; Croner & Kaplan, 1995; Kremers et al., 2004). First, these examples show that marmoset P and M cell responses are consistent with the properties shown in Old World monkey models for human vision (i.e., predominantly macaque monkeys) and, second, that blue-on responses are present in the K layers of marmoset LGN. Population data consistent with these examples, and showing segregation of blue-on responses to K layers, are shown in Fig. 1F and 1G. These data were accumulated from over 20 marmosets. The curved layers of the LGN (Fig. 1F) have been "straightened" (Fig. 1G) and the areas of shaded zones set proportional to the volumes of the P and M layers. Reconstructed depth of cone-opponent cells are shown as leaf plots, where each symbol represents one recorded cell. Blue-on and blue-off cells were present in both dichromatic and trichromatic marmosets (White et al., 2001; Szmajda et al., 2006; Tailby et al., 2008*b*). Red–green opponent cells were only present in trichromatic female marmosets; these receptive fields were segregated to the P layers. Responses of red–green opponent cells are not further considered in the present review but are reviewed elsewhere (Lennie & Movshon, 2005; Jacobs, 2008; Lee et al., 2010; Martin et al., 2011).

In sum, these data show that signals serving distinct (blue–yellow and red–green) axes of color vision in marmosets leave the LGN on distinct anatomical lines. This conclusion is supported by evidence for distinct termination of S-cone signal carrying axons in superficial layers of macaque primary visual cortex (Chatterjee & Callaway, 2003). There is more recent evidence that S-cone signals are segregated to the K system in macaque (Roy et al., 2009). In macaque, the segregation of K layers from P layers is substantially less marked than in marmosets, and some blue-on and blue-off cells are located in "bridges" of K cells spanning the inner P layers (Schiller & Malpeli, 1978), a result consistent with earlier recordings

shading) and magnocellular (M, dark shading) layers and interspersed koniocellular (K) layers. Path of an extracellular recording electrode is shown as a vertical black line and short horizontal lines show locations of recorded cells. Symbols show position of the cells with responses illustrated in **C**, **D**, **E**. (**C**) PSTH of P-off cell response to temporal square wave modulation of a spatially uniform achromatic (left column) and S-cone isolating (center column) fields. Note tonic response to maintained achromatic contrast and negligible response to S-cone modulation. Right column shows contrast-response curve for sinusoidal modulation of the achromatic field. Points show amplitude of fundamental Fourier component (f1) at stimulus frequency. Note linear contrast-response relation. (**D**) Responses of a K blue-on cell in the same format. Note vigorous responses to S-cone modulation. Right column shows response to S-cone isolating modulation. (**E**) Responses of an M-off cell in the same format. Note phasic response to achromatic contrast. Right column shows response to achromatic modulation. Note saturating contrast-response function. Stimulus field diameter (deg)/receptive field eccentricity (deg): P, 8.0/1.5; K, 1.0/0.9; and M, 2.0/8.6. (**F**) Schematic drawing of marmoset LGN showing P and M layers (gray texture) and K layers (blue shading). (**G**) Reconstructed depth of cone-opponent cells. Each symbol represents one recorded cell. Shaded regions represent P and M layers. Note segregation of blue–yellow opponent cells to K layers and red–green opponent cells to P layers. Panels **B**–**E** modified from Cheong et al. (2011). Data for panel F from Martin et al. (1997, 2011). Error bars show standard deviations.

https://doi.org/10.1017/S0952523813000631 Published online by Cambridge University Press

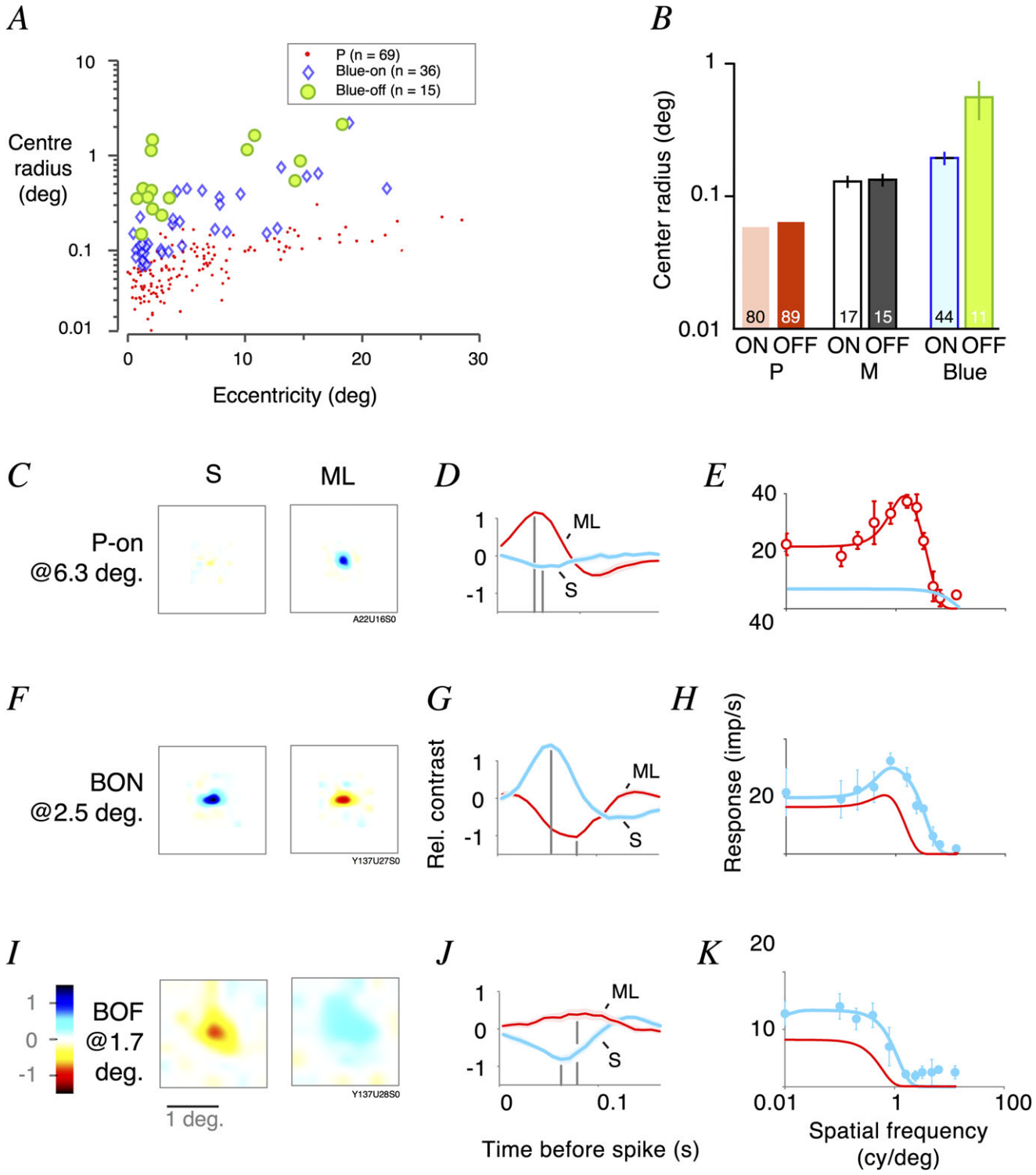


Fig. 2. Characteristics of blue-on and blue-off receptive fields in marmoset LGN. (**A**) Center radius from difference-of-Gaussians fit of responses to drifting S-cone-isolating gratings. Note radius of parvocellular (P) cells is smaller than that of blue-on and blue-off cells at a given eccentricity. (**B**) Mean radius of P cells, magnocellular (M) cells, and blue-on and blue-off receptive fields in central 10 deg. Note that radius of on and off cells is indistinguishable for that of P and M cells, whereas blue-off receptive fields are substantially larger than those of blue-on cells. (**C**, **F**, **I**) Contour maps showing the spike-triggered average stimuli for uniformly distributed, pseudo-randomly presented contrast steps on S-cone-modulating (left column), and ML cone-modulating (right column) axes. Cell class and receptive field eccentricity are shown at left of the S-cone plots. The P cell (**C**) shows weak inhibitory input from S-cones. Note good agreement in the spatial position but distinct response probability profiles of the cone opponent inputs for blue-on (**F**) and blue-off cell (**I**). (**D**, **G**, **J**) Spike-triggered average stimulus timecourse at the spatial location showing the highest ML-cone variance (**D**) of the highest S-cone variance (**G**, **J**). Vertical gray lines indicate peak times. Note that the ML timecourse is slower than the S timecourse for the

https://doi.org/10.1017/S0952523813000631 Published online by Cambridge University Press

(Roy et al., 2009). Finally, three older and one more recent study of cat LGN showed that blue-on cells with properties homologous to those in marmoset and macaque LGN are segregated to the ventral (C, C1, and C2) layers (Pearlman & Daw, 1970; Cleland et al., 1976; Wilson et al., 1976; Buzás et al., 2013). Receptive fields showing spectral opponent properties like blue-on and (less frequently) blue-off cells were recorded in ground squirrel optic nerve and LGN: Michael (1973) found that, in ground squirrel LGN, the blue-on and blue-off cells partially segregated to the outer shell of the nucleus (near the optic tract) but only a small number of cells was studied. Buzás et al. (2013) characterized 14 blue-on cells in cat LGN and found that these cells showed blue-on/yellow-off responses as a result of on-type excitation from S-cones and off-type excitation from medium- to long-wavelength range (ML) cones. The S-on and ML-off components showed considerable overlap, implying that blue-on cells in cats are functionally very similar to blue-on cells in macaque and marmoset monkeys. Blue-on fields were segregated to the ventral (C complex) layers in cat LGN; these layers are rich in nonstandard or "W" type receptive fields (Cleland et al., 1976; Wilson et al., 1976). Taken together, these studies suggest that anatomical segregation of signals arising in S-cones is a common feature in the LGN of primate and nonprimate mammals. Surprisingly, there are to the authors' knowledge no reports on central physiology or distribution of S-cone signals in the thalamus of other mammals.

Spatial properties and anatomical implications

In the foregoing descriptions, blue-on and blue-off receptive fields were distinguished by their strong functional inputs from S-cones. Blue-on cells are excited by S-cone contrast increments; blue-off cells are excited by S-cone contrast decrements. In this section, we discuss the spatial properties of blue-on and blue-off receptive fields. This question bears on the anatomical substrates of S-cone signal-carrying cells in the retina, a topic also treated elsewhere in this issue.

Early studies of spatial properties used hand-held or projected stimuli; for spectral characterization, the illuminant was passed through broad-band (gelatine or polyester based) or narrow-band (interference) filters, and the stimuli were customarily delivered at high contrast on dark backgrounds. Stray light, under such conditions, can bias toward overestimating receptive field size, especially in the central visual field of monkeys where receptive fields are tiny. Despite this problem, there is consensus from early and later studies that blue-on receptive fields are larger than P cell receptive field centers at any given eccentricity. Fig. 2A and 2B compares blue-on, blue-off, and P cell field radius recovered from responses to drifting achromatic (for P cells) or S-cone selective gratings (for blue-on cells), using the venerable difference-of-Gaussians model (Rodieck & Stone, 1965; Enroth-Cugell & Robson, 1966; Croner & Kaplan, 1995). The measurements are consistent with the demonstrated anatomical substrates, whereby blue-on cells get input from small bistratified cells and P cells get input from midget class ganglion cells. In trichromatic monkeys, many P cells (specifically, nearly all P cells near the fovea) show red–green opponent responses because the excitatory center and inhibitory surround mechanism get different medium-wave and long-wave receptor weighting. The question of cone selectivity in P cell fields is reviewed elsewhere (Conway et al., 2010; Lee et al., 2010).

Although a clear picture is given by concordant anatomy and physiology in blue-on cells and P cells, the anatomical picture regarding blue-off cells is murky. Isolated examples of sparse (large-field) ganglion cells showing blue-off responses and large receptive fields were reported from *in vitro* studies of macaque monkey retina (Dacey & Packer, 2003). This result is consistent with recordings from LGN in marmoset and macaque monkeys, where blue-off cells show large receptive fields (Szmajda et al., 2006; Tailby et al., 2008*a*,*b*). However, the reported presence of blue-off responses in parvocellular giant/melanopsin (PGM) cells makes this picture more complex (Dacey et al., 2005). The accepted role of PGM cells in primates and other mammals is their contribution to "non-image-forming" visual functions such as circadian control (*via* projections to suprachiasmatic and pregeniculate nucleus) and pupillary control (*via* projections to the olivary pretectal nucleus; reviewed by Sand et al., 2012). How off-type S-cone inputs to PGM cells (which means PGM activity would be reduced by short-wave light) relate to their non–image-forming role is not clear. On the other hand, the evidence that PGM cells do project to LGN (Rodieck & Watanabe, 1993; Dacey et al., 2003, 2005; Szmajda et al., 2008) suggests that PGM-cell carried signals could reach the cortex and contribute to pathways serving conscious vision. This enigmatic dual role for PGM cells needs further clarification. Of course, any role for PGM cells in conscious vision must be limited by the very low density of PGM cells relative to P and M cells, especially in the fovea.

The question of anatomical basis of blue-off signals in primates is even further complicated by an electron microscopic analysis that reported off-type S-cone connections to five midget bipolar cells in the fovea of one macaque monkey (Klug et al., 2003). This result predicts that there should be tiny (P-size) blue-off receptive fields in the fovea. Yet, such receptive fields have never been reported from over three decades of retinal or LGN recordings. For example, nearly all the blue-off fields within 5 deg of the marmoset fovea are substantially larger than the blue-on fields at the same eccentricity (Fig. 2A) (Szmajda et al., 2006; Tailby et al., 2008*b*). The subtle but important point here is that chromatic aberration cannot fully explain the large field size of purported "blue-off-midget" cells, for blue-on cell fields would likewise be enlarged by out-of-focus short-wave light. This outstanding puzzle is also taken up elsewhere in this issue (Dacey et al., 2013; Miyagishima et al., 2013).

Opponent inputs to blue-on cells

When analyzed using drifting gratings, the small bistratified cells recorded in retina show well-matched and overlapping blue-on and yellow-off receptive field components (Crook et al., 2009; Dacey et al., 2013). Spatiotemporal analysis of blue-on receptive fields

blue-on cell (**G**) and blue-off cell (**J**). (**E**, **H**, **K**) Difference-of-Gaussian fits (lines) to fundamental Fourier component amplitude (points) of responses to drifting cone-selective gratings for these three cells. Note characteristic band-pass response of P cell (**E**) to ML cone isolating gratings (red line). Note the blue-on cell shows low-frequency roll off in the spatial tuning curves for S and ML cone-selective stimuli, and blue-off cell shows low-pass spatial tuning for both conditions. Note that the ML field for this cell is slightly smaller than the S field but on average across blue-on cells, the ML field is slightly larger than the S field. Panels **A**, **B** modified from Tailby et al. (2008*b*). Panels **C**–**K** modified from Martin, Solomon, Tailby, and Cheong (unpublished observations).

https://doi.org/10.1017/S0952523813000631 Published online by Cambridge University Press

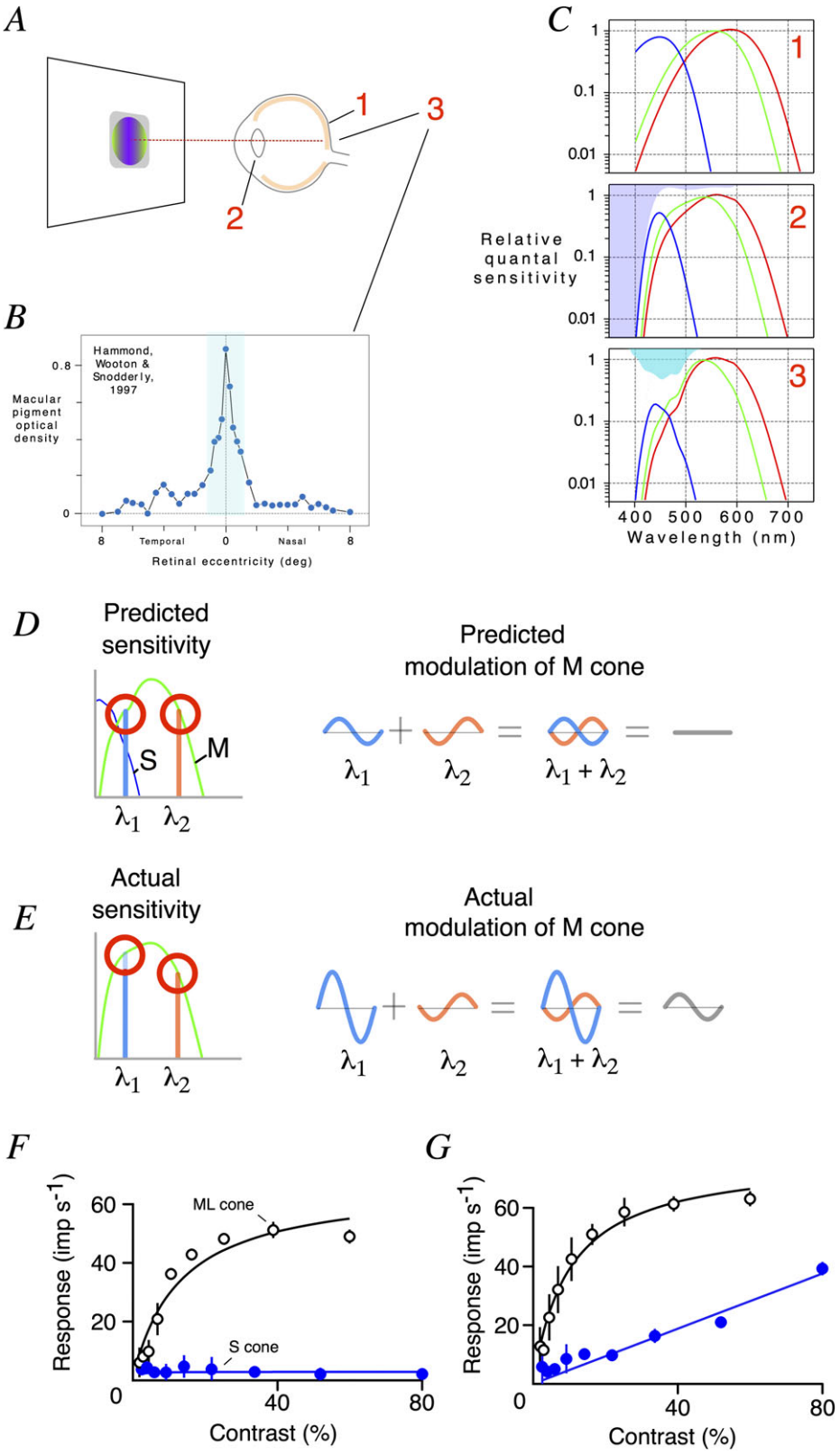


Fig. 3. Predicting and measuring weak S-cone inputs. (**A**) Sketch of the stimulus–eye system showing sites of wavelength-dependent absorption: (1) cone opsins; (2) lens and other optic media; (3) macular pigment and nonopsin retina structures. Cone opsin sensitivity modified by these passive filters is nicknamed "corneal sensitivity". (**B**) Example of eccentricity dependence of macular pigment density in a human subject (modified from Hammond et al., 1997). (**C**) Modification of spectral cone absorbance. Panel 1 shows receptor sensitivities. Panel 2 shows reduction of short-wave receptor sensitivity by lens and other optic media, which absorb light wavelengths below 450 nm (purple shaded region). Panel 3 shows reduction of sensitivity by macular pigments between 400 and 500 nm (cyan shaded region). (**D**) Principle of silent substitution. Two lights (λ_1, λ_2) to which medium-wave sensitive (M) cones are equally sensitive

https://doi.org/10.1017/S0952523813000631 Published online by Cambridge University Press

using reverse correlation analyses in *in vitro* macaque retina, however, showed "hot spots" presumably corresponding to the location of individual S-cones feeding the receptive field (Chichilnisky & Baylor, 1999). Furthermore, this method as well as *in vivo* recordings from macaque retina and marmoset LGN showed that the yellow-off receptive field region is consistently slightly larger (by about 30% of the area) than the blue-on region (Solomon et al., 2005; Field et al., 2007; Tailby et al., 2008*b*). Such deviation from the ideal "Type II" (Wiesel & Hubel, 1966) color-coding organization can have consequences for response of blue-on cells to achromatic stimuli. If the opponent inputs are balanced in functional weight and size, an ideal Type II receptive field will show zero response to achromatic contrast. But blue-on cells stimulated with drifting achromatic gratings can show complex properties, including orientation and direction selectivity as a result of different size, shape and response timing of the blue-on and yellow-off receptive field subunits (Forte et al., 2005; Tailby et al., 2008*a*). These effects are explained in detail elsewhere (Tailby et al., 2010), and for now, the important point is that an experimenter restricted to using achromatic stimuli might find the responses of blue-on cells indecipherable.

Advances in stimulus technology and data processing allow the spatiotemporal structure of receptive fields to be studied in detail, using reverse correlation analysis (Chichilnisky & Baylor, 1999; Field et al., 2007, 2010; Solomon et al., 2010). For example, Fig. 2C–2K shows that the contour maps for a nonopponent P on-centre cell (Fig. 2C), a blue-on cell (Fig. 2F), and a blue-off cell (Fig. 2I) show the spike-triggered average stimuli for uniformly distributed, pseudo-randomly modulated contrast on S-cone-modulating (left column), and ML cone-modulating or "silent S-cone" (right column) axes. As expected, the P cell (Fig. 2C) shows a small ML excitatory region and weak off-sign S-cone input. For the blue-on cell (Fig. 2F) and the blue-off cell (Fig. 2I), there is fair agreement in the spatial position of the cone opponent inputs, but the spatial response profiles are distinct. The spike-triggered average stimulus timecourse for S and ML isolating conditions (Fig. 2D–2J) shows the expected biphasic timecourse for ML excitation in the P cell (Fig. 2D). For the blue-on cell (Fig. 2G) and the blue-off cell (Fig. 2J), the ML timecourse is slower than the S timecourse (for the blue-on cell, the response peaks are separated by over 15 ms). Thus, there are spatial and temporal asymmetries in the opponent inputs to the blue-on and blue-off cells. That the ML input is often weaker than the S input to blue-on and blue-off cells is also shown in the responses to drifting cone-selective gratings (Fig. 2H and 2K). The S and ML inputs to blue-on cells in macaque retina and LGN measured *in vivo* show closely matched temporal properties (Yeh et al., 1995*a*; Solomon et al., 2005; Tailby et al., 2008*a*), but ML delays of 6–20 ms relative to S inputs are reported from *in vitro* recordings (Chichilnisky & Baylor, 1999; Crook et al., 2009). Furthermore, unlike the situation in macaque retina (Crook et al., 2009; Dacey et al., 2013), the blue-on receptive fields in LGN commonly show spatial antagonism in the S-cone inputs, evidenced by a low-frequency roll-off in the spatial tuning curve for S-cone-selective stimuli (Fig. 2H). The centre-surround antagonism in S-cone inputs to blue-on and blue-off cells is however weaker than that exhibited by P cells (Fig 2E; Tailby et al., 2008*a*,*b*).

What is the source of yellow-off opponent inputs to the blue-on receptive fields? As detailed elsewhere in this issue (Dacey et al., 2013; Miyagishima et al., 2013)—in macaque retina, connections from diffuse off-type bipolar cells to the outer tier of small bistratified cells will show yellow-off responses. Inputs to off-bipolar cells are naturally biased against S-cones for the simple reason that S-cones make up less than 10% of the cone population (Marc & Sperling, 1977; Wikler & Rakic, 1990; Martin & Grünert, 1999; Roorda & Williams, 1999). Furthermore, the connections of diffuse bipolar cells with S-cones are weaker than their connections with ML cones (Lee & Grünert, 2007). Contribution of outer retinal (horizontal cell) and inner retina (amacrine cell) inhibition to the blue-on receptive fields in primates is treated in detail elsewhere (Dacey et al., 2013; Miyagishima et al., 2013).

Selectivity and isolation of S-cone signals

So far we have discussed the responses of cells receiving strong inputs from S-cones. Blue-on and blue-off cells are straightforward to identify in a laboratory setting: blue on cells are vigorously excited and blue-off cells are profoundly inhibited, by almost any stimulus which is dominated by short-wave light. A different and more subtle question is cross-talk or "leakage" of S-cone signals to P and M cells (Lee, 2008). Experiments designed to answer this question must take into account the details of spectral absorption in optic media as well as photoreceptor sensitivity and the contrast sensitivity of P and M cells. We explain the process here in some detail, so that newcomers to the field can see how to avoid pitfalls and interpret apparently conflicting results.

Fig. 3A sketches the stimulus-eye system. Before absorption by the receptors, (1) the light passes through (and is partially absorbed by) the lens and other optic media. (2) Light from stimuli close to the visual axis is imaged at the fundus (*macula lutea*, 3), which contains a variable amount of carotenin-based visual pigments (Wyszecki & Stiles, 1982; Snodderly et al., 1984*a*,*b*). The optical density of macular pigment falls sharply with visual field eccentricity (Fig. 3B). The absorption of human S, M, and L cones is sketched in Fig. 3C–panel 1 (Smith & Pokorny, 1975; Stockman et al., 1993; Lamb, 1995). The lens and other optic media (shading, Fig. 3C–panel 2) effectively cut off wavelengths below 400 nm and reduce differentially the sensitivity of S-cones. The macular pigment (shading, Fig. 3C–panel 3) provides absorption in the 400–500 nm range. The effective photoreceptor absorbance (the "corneal sensitivity"), therefore, has a more complex shape than that dictated by the receptor sensitivity alone. Furthermore, every eye is unique: the absorbance characteristics of the lens change

(left panel) are exchanged in sinusoid counterphase (right panel). The predicted modulation of M cone is zero, whereas the modulation of short-wave sensitive (S) cones will be substantial because S-cones are much more sensitive to λ_1 than to λ_2. (**E**) Hazard of silent substitution. If the M cone sensitivity to λ_1 is greater than predicted, the exchange will no longer be silent for the M cone. (**F**, **G**) Example failure of silent substitution. Contrast-response curves showing saturating hyperbolic "Naka–Rushton" fits (lines) and fundamental Fourier component amplitude (points) of one magnocellular cell's responses to nominally cone-selective gratings. Note high gain and saturating responses to ML cone modulation. Cone-selective gratings in (**F**) were produced using appropriate corneal sensitivities for the receptive field, which lay outside fovea. Gratings in (**G**) were produced using foveal corneal sensitivities. Note spurious response to S-cone-selective gratings in (**G**). Responses to maximum S-cone contrast (~35 imp/s) are equivalent to ~5% modulation of M cone.

https://doi.org/10.1017/S0952523813000631 Published online by Cambridge University Press

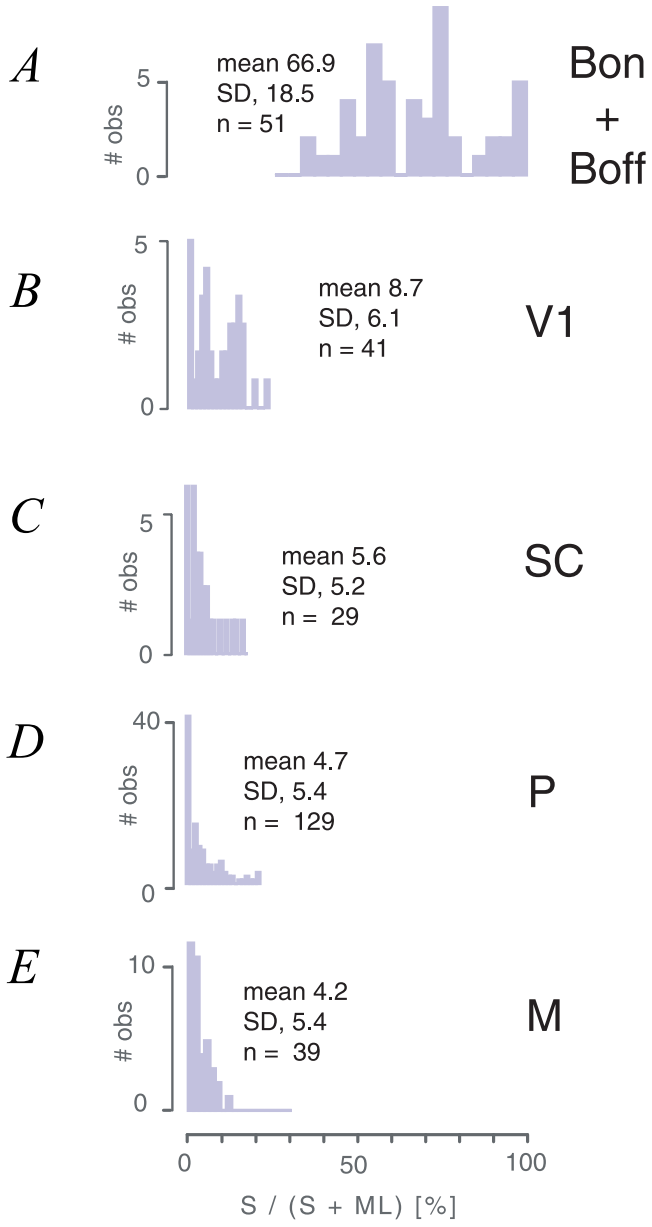


Fig. 4. Comparison of S-cone weights. Each histogram shows the functional weight of S-cone input as a proportion of all cone inputs to the receptive field. (**A**) Blue-on and blue-off fields in LGN. (**B**) Cells in primary visual cortex (V1). (**C**) Cells in superior colliculus (SC). (**D**) Parvocellular (P) cells. (**E**) Magnocellular (M) cells. Note lack of strong S-cone input to cells other than blue-on and blue-off LGN cells.

with age, the density and distribution of macular pigment show great individual variation, the peak sensitivities of cones can vary due to cone opsin polymorphism, and so on. Next, we consider the effect of this unavoidable variation on measurements designed to detect S-cone signals.

Fig. 3D sketches a simplified "silent substitution" experiment. Here, our goal is to modulate S-cones but not M cones. We choose two wavelengths to which M cones are equally sensitive (λ_1, λ_2; Fig. 3D), make their intensities the same, then exchange them, for example, as out-of-phase sinusoids (Fig. 3D). Under this stimulus, the M cone excitation is not changed (the M cone is "silent"), but S-cone excitation will change appreciably because S-cones are much more sensitive to λ_1 than to λ_2. Modulation in a downstream component of the visual pathway should now indicate functional input from S-cones. (The principle shown here for a two-receptor system can be elaborated to three receptors by mixing three lights.) But, now consider the effect of deviation of M cone sensitivity from those predicted by the cone fundamentals (Fig. 3E). If the M cone is more sensitive to λ_1 than to λ_2, the exchange will no longer be silent for the M cone, and the activity in a downstream component of the visual pathway may be wrongly attributed to S-cone inputs.

The problems of silent substitution are most pervasive in recordings of high-gain cells such as magnocellular cells, which act as very sensitive amplifiers of cone contrast. A cautionary example is shown in Fig. 3F and 3G. These contrast-response curves were recorded from a magnocellular cell with a receptive field well outside the fovea, at 14 deg, eccentricity. The high-gain saturating response to ML cone modulation is similar to that shown in Fig. 1E. For properly constructed S-cone isolating gratings, this cell shows no response (Fig. 3F). But in a recording made from the same cell a few minutes later (Fig. 3G), we record a substantial response to S-cone isolating gratings. The difference here is that for Fig. 3G, the S-cone isolating grating was constructed using "wrong" receptor sensitivities (incorporating macular pigment absorption). The resulting deviation from ideal ML cone substitution conditions has caused a small degree of ML cone modulation, which lies at the root of the spurious response. Reported S-cone inputs to magnocellular cells in macaque LGN may be affected by this problem (Chatterjee & Callaway, 2002), although specific S-cone signal injection at LGN level in macaque cannot be ruled out. Parasol cells in macaque retina show no sign of S-cone input when measured with a highly sensitive method, using fundamentals appropriate for the receptive field eccentricity of the cell (Sun et al., 2006*a*,*b*). Likewise, the magnocellular cells in marmoset LGN show negligible S-cone input, that is, below the weight expected from random cone connections (Tailby et al., 2008*b*).

Notwithstanding the technical difficulties outlined above, there is consistent physiological evidence for weak S-cone inputs to the midget-P pathway. In macaque monkeys, functional input from S-cones to midget-P cells is undetectable in recordings from central retina (Sun et al., 2006*a*,*b*). However, Field et al., (2010) identified S-cone inputs to ganglion cells using *in vitro* recordings of peripheral macaque retina. They showed that there is reliably detectable (i.e., nonzero) excitatory S-cone input to off-midget cells (Field et al., 2010). On average, the functional weight of these S-cone inputs to off-midget cells was, however, even lower than the already low proportion (5–10%) expected on the basis of random cone connections. Furthermore, about 40% of S-cones make no contact at all with midget bipolar cells (Field et al., 2010); a result which is consistent with anatomical evidence for sparse connections of S-cones to midget bipolar cells in marmoset retina (Lee et al., 2005). Accordingly, recordings from macaque and marmoset LGN show weak and variable inhibitory S-cone inputs to P cell receptive fields (Tailby et al., 2008*b*). In summary, both anatomical and physiological evidence show that there is functional segregation of S-cone signals toward blue-on and blue-off cells and away from P and M cells.

The pioneering advance made by Field et al. (2010) was to individually stimulate and identify different cones with high spatial resolution stimuli *in vitro*. A conceptually related but technologically distinct approach is to bypass the spatial limitations imposed by natural optics *in vivo.* McMahon et al. (2000) used laser interferometry to study the fine structure of P cell receptive fields in the fovea.

https://doi.org/10.1017/S0952523813000631 Published online by Cambridge University Press

Roorda and Williams (1999) and Sincich et al. (2009) used adaptive optics ophthalmoscopy to show that P cells can respond to stimulation of a single cone photoreceptor. These methods have not yet been combined with spectral analysis to identify cone classes but they have the potential to map chromatic inputs to receptive fields *in vivo* to the level of precision now achievable *in vitro*. A drawback is that both methods require advanced technology currently beyond the reach of most visual neuroscience laboratories.

Distribution of S-cone signals in subcortical and cortical areas

How widespread are S-cone signals among subcortical and cortical targets? The previous sections have shown that within the LGN of marmoset and macaque monkeys, two broad functional groups of on- and off-centre cells with strong S-cone input can been identified, and these cells likely form part of the primitive koniocellular division of the LGN (Hendry & Reid, 2000; Szmajda et al., 2006; Szmajda et al., 2008; Tailby et al., 2008*a*; Roy et al., 2009). Consistently, the likely homologous C complex layers of cat LGN are the target of blue-on cells (Cleland et al., 1976; Buzás et al., 2013). However, in another primitive visual center, the superior colliculus (Fig. 4C), we found no evidence for cells with strong S-cone input. This result is in contrast to evidence for long-latency S-cone inputs to collicular cells recorded in awake macaques. Likewise, recordings from primary visual cortex in (anaesthetized) marmoset and (waking or anaesthetized) macaque consistently show a broader distribution of S-cone inputs to V1 cells than for P and M cells, yet no evidence for a distinct group of cells with S-cone input weight like blue-on and blue-off cells in LGN (DeValois et al., 2000; Solomon et al., 2005; Hashemi-Nezhad et al., 2008). The question of cortical distribution of S-cone signals is taken up again in other chapters of this special issue (Xiao, 2013; also refer the Conway article in this issue). Here, we want to reinforce the fact that the good understanding of the distribution of S-cone signals among retinal and geniculate cells stands in contrast to the limited data available from other subcortical targets in primates.

Acknowledgments

The authors would like to thank their co-workers and students for their invaluable contributions to many of the experiments described here. K. Cheong, S. Solomon, and C. Tailby helped to collect some of the data shown in Fig. 2. Preparation of this review was partially supported by NEI EY13112 (to B.B.L.), NHMRC 1027913 (to P.R.M.), and ARC CE0561903.

References

Buzás, P., Kóbor, P., Petykó, Z., Telkes, I., Martin, P.R. & Lénárd, L. (2013). Receptive field properties of color opponent neurons in the cat lateral geniculate nucleus. *The Journal of Neuroscience* **33**, 1451–1461.

Chatterjee, S. & Callaway, E.M. (2002). S cone contributions to the magnocellular visual pathway in macaque monkey. *Neuron* **35**, 1135–1146.

Chatterjee, S. & Callaway, E.M. (2003). Parallel colour-opponent pathways to primary visual cortex. *Nature* **426**, 668–671.

Cheong, S.K., Tailby, C., Martin, P.R., Levitt, J.B. & Solomon, S.G. (2011). Slow intrinsic rhythm in the koniocellular visual pathway. *Proceedings of the National Academy of Sciences of the United States of America* **108**, 14659–14663.

Cheong, S.K., Tailby, C., Solomon, S.G. & Martin, P.R. (2013). Cortical-like receptive fields in the lateral geniculate nucleus of marmoset monkeys. *The Journal of Neuroscience* **33**, 6864–6876.

Chichilnisky, E.J. & Baylor, D.A. (1999). Receptive-field microstructure of blue-yellow ganglion cells in primate retina. *Nature Neuroscience* **2**, 889–893.

Cleland, B.G., Levick, W.R., Morstyn, R. & Wagner, H.G. (1976). Lateral geniculate relay of slowly-conducting retinal afferents to cat visual cortex. *The Journal of Physiology* **255**, 299–320.

Conway, B.R., Chatterjee, S., Field, G.D., Horwitz, G.D., Johnson, E.N., Koida, K. & Mancuso, K. (2010). Advances in color science: From retina to behavior. *The Journal of Neuroscience* **30**, 14955–14963.

Creutzfeldt, O., Lee, B.B. & Valberg, A. (1986). Colour and brightness signals of parvocellular lateral geniculate neurons. *Experimental Brain Research* **63**, 21–34.

Croner, L.J. & Kaplan, E. (1995). Receptive fields of P and M ganglion cells across the primate retina. *Vision Research* **35**, 7–24.

Crook, J.D., Davenport, C.M., Peterson, B.B., Packer, O.S., Detwiler, P.B. & Dacey, D.M. (2009). Parallel ON and OFF cone bipolar inputs establish spatially coextensive receptive field structure of blue-yellow ganglion cells in primate retina. *The Journal of Neuroscience* **29**, 8372–8387.

Crook, J.M., Lee, B.B., Tigwell, D.A. & Valberg, A. (1987). Thresholds to chromatic spots of cells in the macaque geniculate nucleus as compared to detection sensitivity in man. *The Journal of Physiology* **392**, 193–211.

Dacey, D.M., Crook, J.D. & Packer, O.S. (2013). Distinct synaptic mechanisms create parallel S-ON and S-OFF color opponent pathways in the primate retina. *Visual Neuroscience*, 1–13.

Dacey, D.M., Liao, H.W., Peterson, B.B., Robinson, F.R., Smith, V.C., Pokorny, J., Yau, K.W. & Gamlin, P.D. (2005). Melanopsin-expressing ganglion cells in primate retina signal colour and irradiance and project to the LGN. *Nature* **433**, 749–754.

Dacey, D.M. & Packer, O.S. (2003). Colour coding in the primate retina: Diverse cell types and cone-specific circuitry. *Current Opinion in Neurobiology* **13**, 421–427.

Dacey, D.M., Peterson, B.B., Robinson, F.R. & Gamlin, P.D. (2003). Fireworks in the primate retina: In vitro photodynamics reveals diverse LGN-projecting ganglion cell types. *Neuron* **37**, 15–27.

DeMonasterio, F.M. (1979). Asymmetry of on- and off-pathways of blue sensitive-cones of the retina of macaques. *Brain Research* **166**, 39–48.

DeMonasterio, F.M. & Gouras, P. (1975). Functional properties of ganglion cells of the rhesus monkey retina. *The Journal of Physiology* **251**, 167–195.

DeMonasterio, F.M., Gouras, P. & Tolhurst, D.J. (1975). Trichromatic colour opponency in ganglion cells of the rhesus monkey retina. *The Journal of Physiology* **251**, 197–216.

Derrington, A.M., Krauskopf, J. & Lennie, P. (1984). Chromatic mechanisms in lateral geniculate nucleus of macaque. *The Journal of Physiology* **357**, 241–265.

Derrington, A.M. & Lennie, P. (1984). Spatial and temporal contrast sensitivities of neurones in lateral geniculate nucleus of macaque. *The Journal of Physiology* **357**, 219–240.

DeValois, R.L. (1960). Colour vision mechanisms in monkey. *The Journal of General Physiology* **43**, 115.

DeValois, R.L., Abramov, I. & Jacobs, G.H. (1966). Analysis of response patterns of LGN cells. *Journal of the Optical Society of America* **56**, 966–977.

DeValois, R.L., Cottaris, N.P., Elfar, S.D., Mahon, L.E. & Wilson, J.A. (2000). Some transformations of color information from lateral geniculate nucleus to striate cortex. *Proceedings of the National Academy of Sciences of the United States of America* **97**, 4997–5002.

Diller, L., Packer, O.S., Verweij, J., McMahon, M.J., Williams, D.R. & Dacey, D.M (2004). L and M cone contributions to the midget and parasol ganglion cell receptive fields of macaque monkey retina. *The Journal of Neuroscience* **24**, 1079–1088.

Dreher, B., Fukada, Y. & Rodieck, R.W. (1976). Identification, classification and anatomical segregation of cells with X-like and Y-like properties in the lateral geniculate nucleus of Old-World primates. *The Journal of Physiology* **258**, 433–452.

Enroth-Cugell, C. & Robson, J. (1966). The contrast sensitivity of retinal ganglion cells of the cat. *The Journal of Physiology* **187**, 517–552.

Field, G.D., Gauthier, J.L., Sher, A., Greschner, M., Machado, T.A., Jepson, L.H., Shlens, J., Gunning, D.E., Mathieson, K., Dabrowski, W., Paninski, L., Litke, A.M. & Chichilnisky, E.J. (2010). Functional connectivity in the retina at the resolution of photoreceptors. *Nature* **467**, 673–677.

https://doi.org/10.1017/S0952523813000631 Published online by Cambridge University Press

Field, G.D., Sher, A., Gauthier, J.L., Greschner, M., Shlens, J., Litke, A.M. & Chichilnisky, E.J. (2007). Spatial properties and functional organization of small bistratified ganglion cells in primate retina. *The Journal of Neuroscience* **27**, 13261–13272.

Forte, J.D., Hashemi-Nezhad, M., Dobbie, W.J., Dreher, B. & Martin, P.R. (2005). Spatial coding and response redundancy in parallel visual pathways of the marmoset Callithrix jacchus. *Visual Neuroscience* **22**, 479–491.

Gielen, C.C.A.M., van Gisbergen, J.A.M. & Vendrik, A.J.H. (1982). Reconstruction of cone-system contributions to responses of colour-opponent neurones in monkey lateral geniculate. *Biological Cybernetics* **44**, 211–221.

Gouras, P. (1968). Identification of cone mechanisms in monkey ganglion cells. *The Journal of Physiology* **199**, 533–547.

Hammond, B.R. Jr., Wooten, B.R. & Snodderly, D.M. (1997). Individual variations in the spatial profile of human macular pigment. *Journal of the Optical Society of America A, Optics, Image Science and Vision* **14**, 1187–1196.

Hashemi-Nezhad, M., Blessing, E.M., Dreher, B. & Martin, P.R. (2008). Segregation of short-wavelength sensitive ("blue") cone signals among neurons in the lateral geniculate nucleus and striate cortex of marmosets. *Vision Research* **48**, 2604–2614.

Hendry, S.H.C. & Reid, R.C. (2000). The koniocellular pathway in primate vision. *Annual Review of Neuroscience* **23**, 127–153.

Hubel, D.H. & Wiesel, T.N. (1960). Receptive fields of optic nerve fibres in the spider monkey. *The Journal of Physiology* **154**, 572–580.

Hunt, D.M. & Peichl, L. (2013). S cones: Evolution, retinal distribution, development, and spectral sensitivity. *Visual Neuroscience*, 1–24.

Jacobs, G.H. (2008). Primate color vision: A comparative perspective. *Visual Neuroscience* **25**, 619–633.

Kaas, J.H., Huerta, M.F., Weber, J.T. & Harting, J.K. (1978). Patterns of retinal terminations and laminar organization of the lateral geniculate nucleus of primates. *The Journal of Comparative Neurology* **182**, 517–554.

Kaplan, E. & Shapley, R.M. (1986). The primate retina contains two types of ganglion cells, with high and low contrast sensitivity. *Proceedings of the National Academy of Sciences of the United States of America* **83**, 2755–2757.

Kilavik, B.E., Silveira, L.C. & Kremers, J. (2003). Centre and surround responses of marmoset lateral geniculate neurones at different temporal frequencies. *The Journal of Physiology* **546**, 903–919.

Klug, K., Herr, S., Ngo, I.T., Sterling, P. & Schein, S. (2003). Macaque retina contains an S-cone OFF midget pathway. *The Journal of Neuroscience* **23**, 9881–9887.

Kremers, J., Weiss, S. & Silveira, L.C. (2004). Spatiotemporal properties of the magno and parvocellular neurons of the lateral geniculate nucleus of the marmoset (Callithrix jacchus). *Neurociências* **1**, 138–149.

Lamb, T.D. (1995). Photoreceptor spectral sensitivities: Common shape in the long-wavelength region. *Vision Research* **35**, 3083–3091.

Lee, B.B. (2008). Neural models and physiological reality. *Visual Neuroscience* **25**, 231–241.

Lee, B.B., Martin, P.R. & Grünert, U. (2010). Retinal connectivity and primate vision (review). *Progress in Retinal and Eye Research* **29**, 622–639.

Lee, B.B., Shapley, R.M., Hawken, M.J. & Sun, H. (2012). Spatial distributions of cone inputs to cells of the parvocellular pathway investigated with cone-isolating gratings. *Journal of the Optical Society of America A, Optics, Image Science, and Vision* **29**, A223–A232.

Lee, B.B., Valberg, A., Tigwell, D.A. & Tryti, J. (1987). An account of responses of spectrally opponent neurons in macaque lateral geniculate nucleus to successive contrast. *Proceedings of the Royal Society of London. Series B* **230**, 293–314.

Lee, B.B., Virsu, V. & Elepfandt, A. (1983). Cell responses in dorsal layers of macaque lateral geniculate nucleus as a function of intensity and wavelength. *Journal of Neurophysiology* **50**, 849–863.

Lee, S.C.S. & Grünert, U. (2007). Connections of diffuse bipolar cells in primate retina are biased against S-cones. *The Journal of Comparative Neurology* **502**, 126–140.

Lee, S.C.S., Telkes, I. & Grünert, U (2005). S-cones do not contribute to the OFF-midget pathway in the retina of the marmoset, Callithrix jacchus. *The European Journal of Neuroscience* **22**, 437–447.

Lennie, P. & Movshon, J.A. (2005). Coding of color and form in the geniculostriate visual pathway. *Journal of the Optical Society of America A, Optics and Image Science and Vision* **22**, 2013–2033.

Malpeli, J.G. & Schiller, P.H. (1978). Lack of blue OFF-center cells in the visual system of the monkey. *Brain Research* **141**, 385–389.

Marc, R.E. & Sperling, H.G. (1977). Chromatic organization of primate cones. *Science* **196**, 454–456.

Martin, P.R., Blessing, E.M., Buzás, P., Szmajda, B.A. & Forte, J.D. (2011). Transmission of colour and acuity signals by parvocellular cells in marmoset monkeys. *The Journal of Physiology* **589**, 2795–2812.

Martin, P.R. & Grünert, U. (1999). Analysis of the short wavelength sensitive ("blue") cone mosaic in the primate retina: A comparison of new world and old world monkeys. *The Journal of Comparative Neurology* **406**, 1–14.

Martin, P.R., White, A.J.R., Goodchild, A.K., Wilder, H.D. & Sefton, A.E. (1997). Evidence that blue-on cells are part of the third geniculocortical pathway in primates. *The European Journal of Neuroscience* **9**, 1536–1541.

McMahon, M.J., Lankheet, M.J.M., Lennie, P. & Williams, D.R. (2000). Fine structure of parvocellular receptive fields in the primate fovea revealed by laser interferometry. *The Journal of Neuroscience* **20**, 2043–2053.

Michael, C.R. (1973). Opponent-color and opponent-contrast cells in lateral geniculate nucleus of the ground squirrel. *Journal of Neurophysiology* **36**, 536–550.

Miyagishima, K.J., Grünert, U. & Li, W. (2013). Processing of S-cone signals in the inner plexiform layer of the mammalian retina. *Visual Neuroscience*, 1–13.

Mollon, J.D. (1989). "Tho' she kneel'd in the place where they grew…" The uses and origins of primate colour vision. *The Journal of Experimental Biology* **146**, 21–38.

Nathans, J. (1999). The evolution and physiology of human color vision: Insights from molecular genetic studies of visual pigments. *Neuron* **24**, 299–312.

Pearlman, A.L. & Daw, N.W. (1970). Opponent color cells in the cat lateral geniculate nucleus. *Science* **167**, 84–86.

Reid, R.C. & Shapley, R.M. (2002). Space and time maps of cone photoreceptor signals in macaque lateral geniculate nucleus. *The Journal of Neuroscience* **22**, 6158–6175.

Rodieck, R.W. (1991). Which cells code for color? In *From Pigments to Perception: Advances in Understanding Visual Processes*, ed. Valberg, A. & Lee, B.B., pp. 83–93. London: Plenum Press.

Rodieck, R.W. & Stone, J. (1965). Analysis of receptive fields of cat retinal ganglion cells. *Journal of Neurophysiology* **28**, 833–849.

Rodieck, R.W. & Watanabe, M. (1993). Survey of the morphology of macaque retinal ganglion cells that project to the pretectum, superior colliculus, and parvicellular laminae of the lateral geniculate nucleus. *The Journal of Comparative Neurology* **338**, 289–303.

Roorda, A. & Williams, D.R. (1999). The arrangement of the three cone classes in the living human eye. *Nature* **397**, 520–522.

Roy, S., Martin, P.R., Dreher, B., Saalmann, Y.B., Hu, D. & Vidyasagar, T.R. (2009). Segregation of short-wavelength sensitive (S) cone signals in the macaque dorsal lateral geniculate nucleus. *The European Journal of Neuroscience* **30**, 1517–1526.

Sand, A., Schmidt, T.M. & Kofuji, P. (2012). Diverse types of ganglion cell photoreceptors in the mammalian retina. *Progress in Retinal and Eye Research* **31**, 287–302.

Schiller, P.H. & Malpeli, J.G. (1978). Functional specificity of lateral geniculate nucleus laminae of the rhesus monkey. *Journal of Neurophysiology* **41**, 788–797.

Shyue, S.K., Hewett-Emmett, D., Sperling, H.G., Hunt, D.M., Bowmaker, J.K., Mollon, J.D. & Li, W.H. (1995). Adaptive evolution of color vision genes in higher primates. *Science* **269**, 1265–1267.

Sincich, L.C., Zhang, Y., Tiruveedhula, P., Horton, J.C. & Roorda, A. (2009). Resolving single cone inputs to visual receptive fields. *Nature Neuroscience* **12**, 967–969.

Smith, V.C. & Pokorny, J. (1975). Spectral sensitivity of the foveal cone photopigments between 400 and 500 nm. *Vision Research* **15**, 161–171.

Snodderly, D.M., Auran, J.D. & Delori, F.C. (1984*a*). The macular pigment. II. Spatial distribution in primate retinas. *Investigative Ophthalmology & Visual Science* **25**, 674–685.

Snodderly, D.M., Brown, P.K., Delori, F.C. & Auran, J.D. (1984*b*). The macular pigment. I. Absorbance spectra, localization, and discrimination from other yellow pigments in primate retinas. *Investigative Ophthalmology & Visual Science* **25**, 660–673.

Solomon, S.G., Lee, B.B., White, A.J., Rüttiger, L. & Martin, P.R. (2005). Chromatic organization of ganglion cell receptive fields in the peripheral retina. *The Journal of Neuroscience* **25**, 4527–4539.

Solomon, S.G., Tailby, C., Cheong, S.K. & Camp, A.J. (2010). Linear and non-linear contributions to the visual sensitivity of neurons in primate lateral geniculate nucleus. *Journal of Neurophysiology* **104**, 1884–1898.

https://doi.org/10.1017/S0952523813000631 Published online by Cambridge University Press

Stockman, A., MacLeod, D.I. & Johnson, N.E. (1993). Spectral sensitivities of the human cones. *Journal of the Optical Society of America A, Optics and Image Science and Vision* **10**, 2491–2521.

Sun, H., Smithson, H.E., Zaidi, Q. & Lee, B.B. (2006*a*). Do magnocellular and parvocellular ganglion cells avoid short-wavelength cone input? *Visual Neuroscience* **23**, 441–446.

Sun, H., Smithson, H.E., Zaidi, Q. & Lee, B.B. (2006*b*). Specificity of cone inputs to macaque retinal ganglion cells. *Journal of Neurophysiology* **95**, 837–849.

Szmajda, B.A., Buzás, P., FitzGibbon, T. & Martin, P.R. (2006). Geniculocortical relay of blue-off signals in the primate visual system. *Proceedings of the National Academy of Sciences of the United States of America* **103**, 19512–19517.

Szmajda, B.A., Martin, P.R. & Grünert, U. (2008). Retinal ganglion cell inputs to the koniocellular pathway. *The Journal of Comparative Neurology* **510**, 251–268.

Tailby, C., Dobbie, W.J., Hashemi-Nezhad, M., Forte, J.D. & Martin, P.R. (2010). Receptive field asymmetries produce color-dependent direction selectivity in primate lateral geniculate nucleus. *Journal of Vision* **10**, 1–18.

Tailby, C., Solomon, S.G. & Lennie, P. (2008*a*). Functional asymmetries in visual pathways carrying S-cone signals in macaque. *The Journal of Neuroscience* **28**, 4078–4087.

Tailby, C., Szmajda, B.A., Buzás, P., Lee, B.B. & Martin, P.R. (2008*b*). Transmission of blue (S) cone signals through the primate lateral geniculate nucleus. *Journal of Physiology* **586**, 5947–5967.

Tovée, M.J., Bowmaker, J.K. & Mollon, J.D. (1992). The relationship between cone pigments and behavioural sensitivity in a New World monkey (Callithrix jacchus jacchus). *Vision Research* **32**, 867–878.

Valberg, A., Lee, B.B. & Tigwell, D.A. (1986). Neurones with strong inhibitory s-cone inputs in the macaque lateral geniculate nucleus. *Vision Research* **26**, 1061–1064.

Walls, G.L. (1953). *The Lateral Geniculate Nucleus and Visual Histophysiology*. University of California Press, Berkeley.

White, A.J.R., Solomon, S.G. & Martin, P.R. (2001). Spatial properties of koniocellular cells in the lateral geniculate nucleus of the marmoset Callithrix jacchus. *The Journal of Physiology* **533**, 519–535.

Wiesel, T.N. & Hubel, D.H. (1966). Spatial and chromatic interactions in the lateral geniculate body of the rhesus monkey. *Journal of Neurophysiology* **29**, 1115–1156.

Wikler, K.C. & Rakic, P. (1990). Distribution of photoreceptor subtypes in the retina of diurnal and nocturnal primates. *The Journal of Neuroscience* **10**, 3390–3401.

Wilson, P.D., Rowe, M.H. & Stone, J. (1976). Properties of relay cells in cat's lateral geniculate nucleus: A comparison of W-cells with X- and Y-cells. *Journal of Neurophysiology* **39**, 1193–1209.

Wyszecki, G. & Stiles, W.S. (1982). *Color Science: Concepts and Methods, Quantitative Data and Formulae*. New York: Wiley.

Xiao, Y. (2013). Processing of the S-cone signals in the early visual cortex of primates. *Visual Neuroscience*, 1–7.

Yeh, T., Lee, B.B. & Kremers, J. (1995*a*). Temporal response of ganglion cells of the macaque retina to cone-specific modulation. *Journal of the Optical Society of America A Optics, Image Science, and Vision* **12**, 456–464.

Yeh, T., Lee, B.B., Kremers, J., Cowing, J.A., Hunt, D.M., Martin, P.R. & Troy, J.B. (1995*b*). Visual responses in the lateral geniculate nucleus of dichromatic and trichromatic marmosets (Callithrix jacchus). *The Journal of Neuroscience* **15**, 7892–7904.

https://doi.org/10.1017/S0952523813000631 Published online by Cambridge University Press